Advances in Aircraft and Spacecraft Science, *Vol. 3, No. 3 (2016) 351-366*
DOI: http://dx.doi.org/10.12989/aas.2016.3.3.351

Effects of macroporosity and double porosity on noise control of acoustic cavity

C. Sujatha* and Shantanu S. Kore[a]

Machine Design Section, Department of Mechanical Engineering, Indian Institute of Technology Madras, Chennai 600 036, India

(Received June 3, 2015, Revised September 9, 2015, Accepted September 21, 2015)

Abstract. Macroperforations improve the sound absorption performance of porous materials in acoustic cavities and in waveguides. In an acoustic cavity, enhanced noise reduction is achieved using porous materials having macroperforations. Double porosity materials are obtained by filling these macroperforations with different poroelastic materials having distinct physical properties. The locations of macroperforations in porous layers can be chosen based on cavity mode shapes. In this paper, the effect of variation of macroporosity and double porosity in porous materials on noise reduction in an acoustic cavity is presented. This analysis is done keeping each perforation size constant. Macroporosity of a porous material is the fraction of area covered by macro holes over the entire porous layer. The number of macroperforations decides macroporosity value. The system under investigation is an acoustic cavity having a layer of poroelastic material rigidly attached on one side and excited by an internal point source. The overall sound pressure level (SPL) inside the cavity coupled with porous layer is calculated using mixed displacement-pressure finite element formulation based on Biot-Allard theory. A 32 node, cubic polynomial brick element is used for discretization of both the cavity and the porous layer. The overall SPL in the cavity lined with porous layer is calculated for various macroporosities ranging from 0.05 to 0.4. The results show that variation in macroporosity of the porous layer affects the overall SPL inside the cavity. This variation in macroporosity is based on the cavity mode shapes. The optimum range of macroporosities in poroelastic layer is determined from this analysis. Next, SPL is calculated considering periodic and nodal line based optimum macroporosity. The corresponding results show that locations of macroperforations based on mode shapes of the acoustic cavity yield better noise reduction compared to those based on nodal lines or periodic macroperforations in poroelastic material layer. Finally, the effectiveness of double porosity materials in terms of overall sound pressure level, compared to equivolume double layer poroelastic materials is investigated; for this the double porosity material is obtained by filling the macroperforations based on mode shapes of the acoustic cavity.

Keywords: macroperforations; macroporosity; double porosity; cavity mode shapes; finite element method

1. Introduction

*Corresponding author, Professor, E-mail: sujatha@iitm.ac.in
[a]M.S. Scholar, E-mail: shantanu68.kore@gmail.com

http://www.techno-press.org/?journal=aas&subpage=7 ISSN: 2287-528X (Print), 2287-5271 (Online)

Sound absorbing materials play an important role in noise control inside an enclosure in many industrial applications such as automobiles, aircraft fuselage and buildings. Poroelastic materials such as glasswool, foam and fibreglass dissipate acoustic energy by acoustic wave absorption. These poroelastic materials add extra mass to the system, which is undesirable in applications such as aircraft fuselage where weight reduction is of utmost importance while designing the system. In this respect a noise control system which functions well with lesser weight is favourable.

Biot first studied and developed a theory explaining behaviour of waves in fluid saturated porous media; later Allard applied it to the acoustic domain by characterising wave propagation in poroelastic materials (Allard and Atalla 2009). Since it is difficult to develop a practical and accurate analytical model for poroelastic materials, many researchers have developed different numerical models to predict the behaviour of waves in fluid saturated poroelastic media. Goransson (1995) developed a 4 degree of freedom (dof) mixed solid displacement and pore fluid pressure (u, p) formulation; however he neglected elastic coupling. Earlier several authors had developed mixed formulations, neglecting inertia coupling and making it unsuitable for acoustic applications. Atalla *et al.* (1998) have developed mixed (u, p) formulations which handle coupling conditions naturally. There are various approaches followed to develop numerical models for poroelastic materials, but very few efforts have been reported to increase absorption performance of these materials. Besset and Ichchou (2011) proposed an energy method for optimizing the location of poroelastic materials near walls of an acoustic cavity to improve noise reduction inside the acoustic cavity. Ih *et al.* (2011) in their investigation applied effective independence (EFl) method to determine optimal locations of sources, as well as sound absorbing materials near walls of an acoustic cavity. Totaro and Guyader (2011) developed a technique based on patch transfer function method to optimize the locations of sound absorbing materials on near walls of an irregularly shaped acoustic cavity. They demonstrated effectiveness of optimal distribution over arbitrary distribution of sound absorbing material on the walls of a cavity in reducing noise level. Atalla *et al.* (2001) used geometric modifications in terms of macroperforations and Sgard *et al.* (2005) developed design rules for macroperforations to improve sound absorption performance of poroelastic materials. However these analyses are made in waveguide environment. Babu and Padmanabhan (2010) demonstrated the effectiveness of mode shape based macroperforation patterns to control noise inside a rectangular acoustic cavity.

The present paper examines the effect of variation of macroporosity and double porosity on noise control in terms of overall sound pressure level (SPL) inside an acoustic cavity. At first a finite element model of the system under investigation is presented, followed by its validation with an example available in existing literature. Next, results are discussed illustrating the effects of variation of macroporosity in poroelastic layer on noise control inside the cavity based on the acoustic cavity mode shapes. The optimum range of macroporosity values is determined using this analysis. Next, effectiveness of macroperforations based on cavity mode shapes as compared to periodic and nodal line based macroperforations is investigated. Finally, effectiveness of double porosity over equivolume double layer poroelastic material in terms of overall SPL is presented in this paper.

2. Description of the system

The system under investigation consists of air saturated, isotropic poroelastic material rigidly attached to one of the walls of the acoustic cavity. The dimensions of the acoustic cavity, along

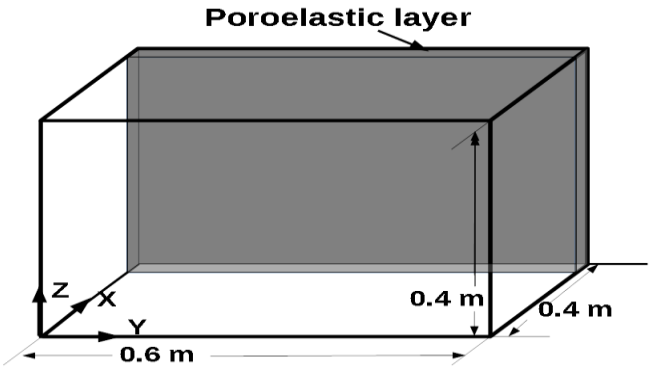

Fig. 1 Acoustic cavity coupled with poroelastic layer

Table 1 Physical properties of materials

Property	Glasswool	Fibreglass	Foam A	Foam B
Porosity h	0.94	0.95	0.97	0.99
Tortuosity α	1.06	1.8	2.52	1.98
Flow resistivity, σ (Nm^{-4})	40000	25000	87000	65000
Viscous characteristic length, Λ (m)	0.56×10^{-4}	0.93×10^{-4}	0.37×10^{-4}	0.37×10^{-4}
Thermal characteristic length, Λ' (m)	1.10×10^{-4}	0.93×10^{-4}	1.19×10^{-4}	1.21×10^{-4}
Shear modulus N (kPa)	2.2×10^{-3}	21	55	15
Frame structural damping, η	0.1	0.05	0.55	0.1
Mass density of frame, ρ_1 (kg/m^3)	130	30	31	16
Poisson's ratio	0	0	0.3	0.3

with the coordinate system are shown in Fig. 1. The cavity is excited by a monopole harmonic point source of strength 0.1 m^3/s^2. Two different excitation locations are considered for the present analysis.

The theory used to predict the behaviour of fluid (air) saturated porous materials under acoustic excitation is based on the work of Biot-Allard (Allard and Atalla 2009). The acoustic cavity and porous layer are modelled using finite element method (FEM). The finite element model consists of three solid phase displacements and pore pressure as field variables. The physical properties of the porous material under consideration (glasswool) are taken from existing literature (Atalla, 1998) and are shown in Table 1.

3. Finite element model of the system

Conventional FEM is used to model the system under study. To discretize the cavity as well as the poroelastic domains, 32-node, isoparametric brick element is used. The shape functions determined from serendipity approach are taken from Zienkiewicz and Taylor (1989). This higher order cubic brick element ensures convergence with a very small number of elements as compared to linear or quadratic brick elements. The present FEM is implemented in MATLAB™.

3.1 Acoustic cavity domain model

The conventional FEM is used to model the acoustic cavity. The detailed description of the formulation can be obtained from Petyt *et al.* (1976). After the discretization of the acoustic cavity with 3-D brick elements, global finite elemental form is given as

$$\{[\mathrm{H}] - \omega^2[\mathrm{Q}]\}[\mathrm{P_a}] = [\mathrm{F_a}] \tag{1}$$

Here [H] and [Q] are kinetic and compression energy matrices respectively and $[P_a]$ and $[F_a]$ are global nodal pressure and acoustic load vector; ω is the natural frequency of the acoustic cavity.

3.2 Poroelastic domain model

The part of the system consisting of poroelastic domain is modelled using mixed pressure-displacement finite element formulation, a detailed description of which can be got from the paper by Atalla *et al.* (1998). This formulation converts the system of poroelastic domain having 6 dof per node to one having 4 dof per node by expressing fluid phase displacement (U) in terms of interstitial pressure (p) in pores. This formulation eventually simplifies spectral analysis due to the natural coupling between poroelastic and acoustic domains, leading to minimisation of the computational cost and time. Here, the same 3-D brick element is used to discretize the poroelastic domain. Finally, global finite element form becomes

$$\begin{pmatrix} [\mathrm{K}] - \omega^2[\overline{M}] & -[\overline{C}] \\ [\overline{C}] & [\overline{H}] - \omega^2[\overline{Q}] \end{pmatrix} \begin{pmatrix} u_n \\ p_n \end{pmatrix} = \begin{pmatrix} F_u \\ F_p \end{pmatrix} \tag{2}$$

Here F_u and F_p form a global loading vector and u_p and p_n constitute global nodal, displacement and pressure variable vectors respectively. $[\overline{H}]$ and $[\overline{Q}]$ are kinetic and compression energy matrices for fluid phase and $[\overline{C}]$ is the volume coupling matrix between solid and fluid phases. [K] and $[\overline{M}]$ are equivalent stiffness and mass matrices for solid phase. The bar symbol indicates that corresponding matrices are complex and frequency dependent. The detailed description of this finite element formulation can be obtained from Atalla *et al.* (1998).

$$\sigma^t.n = -p_a.n$$

$$p = p_a$$

$$(1-h)u.n + hU.n = \frac{1}{\rho_a \omega^2}\nabla p_a.n \tag{3}$$

Here h is the porosity of poroelastic material, ρ_a is air density, P_a is acoustic pressure, σ^t is stress tensor and n is the unit normal vector. The first and second equations represent continuity of normal stress in poroelastic and acoustic cavity domains where acoustic pressure p_a is expressed in terms of normal stress σ^t while the last equation gives continuity in normal volume velocity.

3.3 Model validation

The finite element model is validated with examples from existing literature: 1. Surface

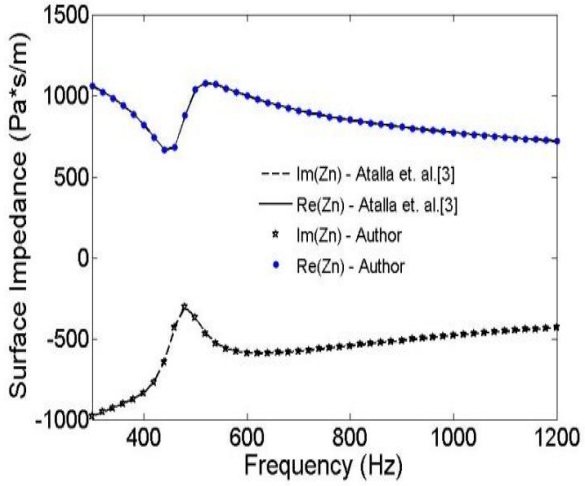

Fig. 2 Surface impedance of laterally infinite Glasswool layer

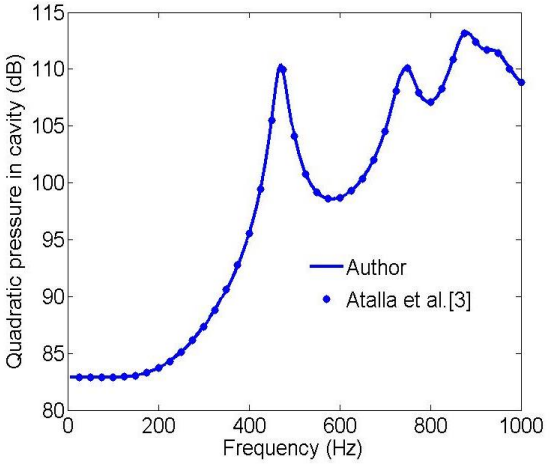

Fig. 3 Mean quadratic pressure inside acoustic cavity

impedance of laterally infinite single glasswool layer and 2. Mean quadratic pressure inside a rigid acoustic cavity.

3.3.1 Surface impedance of single glasswool layer

A laterally infinite single glasswool layer bonded onto a rigid wall is considered. Here, only axial macroscopic displacements are considered to model lateral infiniteness of glasswool layer. The surface impedance for unit normal incidence pressure is given as

$$Z_n = \frac{1}{j\omega(hU_n + (1-h)u_n)} \tag{3}$$

Here subscript n denotes normal displacements. The real and imaginary parts of surface impedance which describe the characteristic behaviour of the material under excitation are shown in Fig. 2, which shows good agreement with the results of Atalla *et al*. (1998)

3.3.2 Mean quadratic pressure inside rigid acoustic cavity

To validate acoustic and poroelastic domain coupling, mean quadratic pressure inside a 3-D acoustic cavity of dimensions 0.1×0.35×0.22 m in X×Y×Z directions is determined. A fibreglass layer of 0.01m thickness is rigidly attached to one of the walls of the cavity. This cavity is excited by a point source positioned at its corner. The comparison of mean quadratic pressure determined by the authors and Atalla *et al.* (1998) is shown in Fig. 3. It shows good agreement between the two. Both the results shown in Fig. 2 and Fig. 3 confirm the validity of the model under study.

4. Results

The effects of variation of macroporosity in poroelastic material layer are investigated by using the system shown in Fig. 1. This system is discretized into 10×7×5 elements using 32 node cubic

order brick element. This discretization shows sufficient convergence. Overall SPL is considered as a parameter to study the performance of the system and can be given as

$$\text{Overall SPL (dB)} = 10 \times \log_{10} \left\{ \frac{\left| \sum_{i=1}^{N} \frac{p_i^2}{2N} \right|}{p_{ref.}^2} \right\} \tag{4}$$

where P_{ref} =20×10^{-4} N/m^2 and N is the number of control (nodal) points in the acoustic domain; p_i is the nodal pressure in acoustic domain (Panneton and Atalla 1997). The overall SPL inside the acoustic cavity is calculated for 40mm and 80mm thickness of poroelastic layer without any macroperforations. The coordinates of two different point source locations considered to excite the acoustic cavity harmonically are shown in Table 2. The comparison of SPLs inside the acoustic cavity with first excitation location PS1 for various thicknesses of poroelastic layer is shown in Fig. 4 and Fig. 5, showing a comparable reduction in SPL with increase in thickness of the layer. Fig. 5 also shows overall SPL (green colour) obtained when the acoustic cavity is excited with PS2.

4.1 Effects of variation of macroprosity in poroelastic layer on overall SPL

In order to examine the effect of variation of macroporosity in poroelastic layer on SPL inside

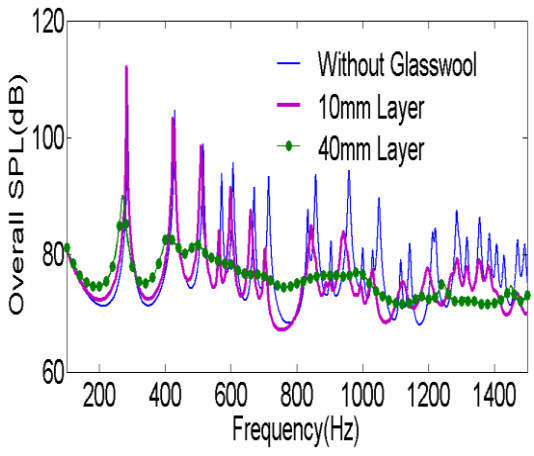

Fig. 4 Overall SPL inside the cavity with 10 mm and 40 mm thickness of Glasswool

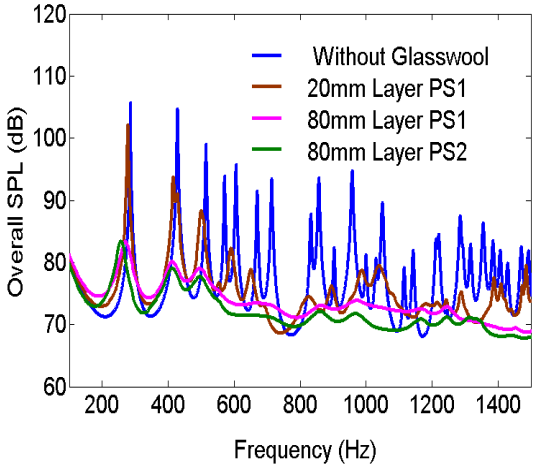

Fig. 5 Overall SPL inside the cavity with 20 mm and 50 mm thickness of Glasswool

Table 2 Coordinates of excitation locations

Excitation locations no.	Coordinates (m)		
	X	*Y*	*Z*
Point source 1 (PS1)	0.30	0.17	0.32
Point source 2 (PS2)	0.2	0.17	0.10

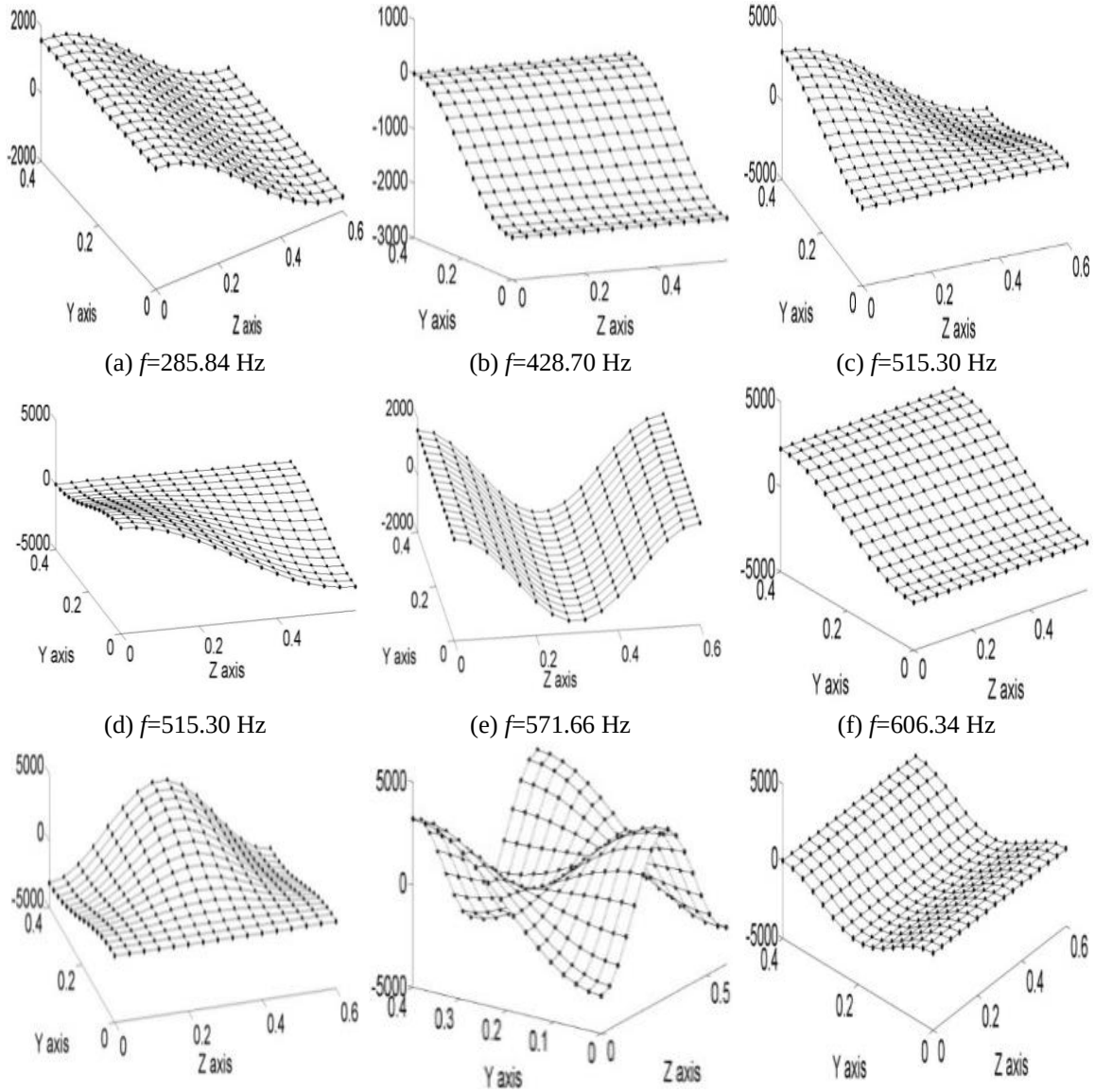

(a) *f*=285.84 Hz (b) *f*=428.70 Hz (c) *f*=515.30 Hz

(d) *f*=515.30 Hz (e) *f*=571.66 Hz (f) *f*=606.34 Hz

(g) *f*=714.60 Hz (h) *f*=833.35 Hz (i) *f*=857.50 Hz

Fig. 6 Different mode shapes of the acoustic cavity in terms of pressure on the surface *YZ* at *X*=0.4 m and corresponding natural frequencies

the acoustic cavity, a certain approach such as periodic, random or mode shape based material removal (macroperforations) has to be followed. It has been shown that mode shape based pattern of macroperforations significantly reduces SPL inside the acoustic cavity (Babu and Padmanabhan 2010). The present paper analyses the effect of variation of these macroperforations based on mode shapes of the acoustic cavity.

Some of the different natural frequencies of the rigid acoustic cavity and corresponding acoustic mode shapes (acoustic pressure patterns) at the surface *YZ* at *X*=0.4 m are shown in Fig.

6. The same finite element model as before is used for this modal analysis. Standard air properties ρ_a=1.23 kg/m^3 and sonic velocity c_a=343 m/s are considered. These pressure acoustic mode shapes are used to locate the macroperforations. From the different mode shapes shown in Fig. 6, it is clear that for most of the modes maximum and minimum values of acoustic pressure occur at the edges of the surface upto the 8th mode which has a natural frequency of 714.60 Hz. These locations at the surface where maximum and minimum values of nodal pressures occur in the pressure acoustic mode shapes are used to locate the positions of macroperforations in the poroelastic layer.

Macroperforations in the poroelastic layer are made by replacing the poroelastic material patch with air. In the present analysis, rectangular shaped macroperforations of volume 80×85×t mm are considered, where *t* is the thickness of the poroelastic layer. This volume of macroperforations is constant throughout the analysis. The macroporosity of the porous material is the fraction of area covered by macroperforations over the entire porous layer. The present poroelastic layer is divided into 35 rectangles having equal area. The number of macroperforations (*M*) decides the value of macroporosity ($\emptyset$). Fig. 7 shows different macroperforation patterns with different values of macroporosity, for example, Pattern 4 (*M*=8) has 8 macroperforations; this makes $\emptyset = \frac{8}{35}$=0.22. In the same manner, all the other macroporosity ($\emptyset$) values are determined. The effect of variation of macroporosity in poroelastic material in terms of sound absorbing coefficient has been investigated by Atalla *et al.* (1998). It can be observed from these results that macroporosity within the range of 0.11 to 0.36 significantly enhances sound absorbing coefficient in mid to high frequency range.

The objective of the present paper is to determine the optimum range of macroporosity values within which a significant reduction in SPL can be achieved within a certain range of frequencies. Further, the number of macroperforations decide the value of macroporosity. Using this, detailed

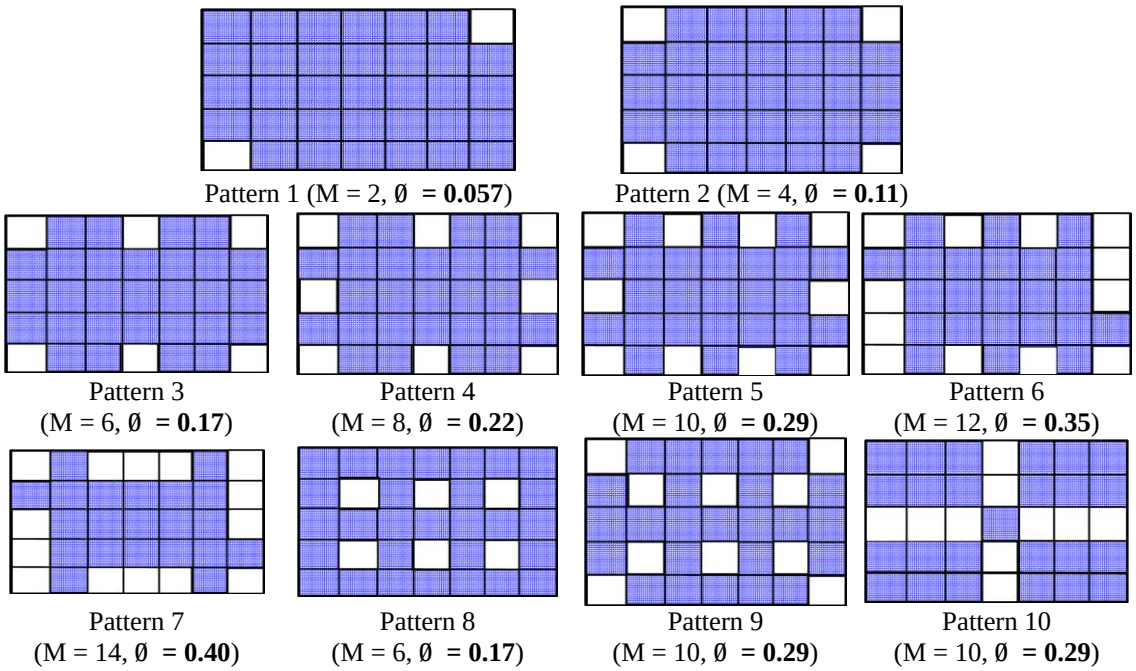

Fig. 7 (b) Macroperforation patterns with various macroporosity ($\emptyset$)

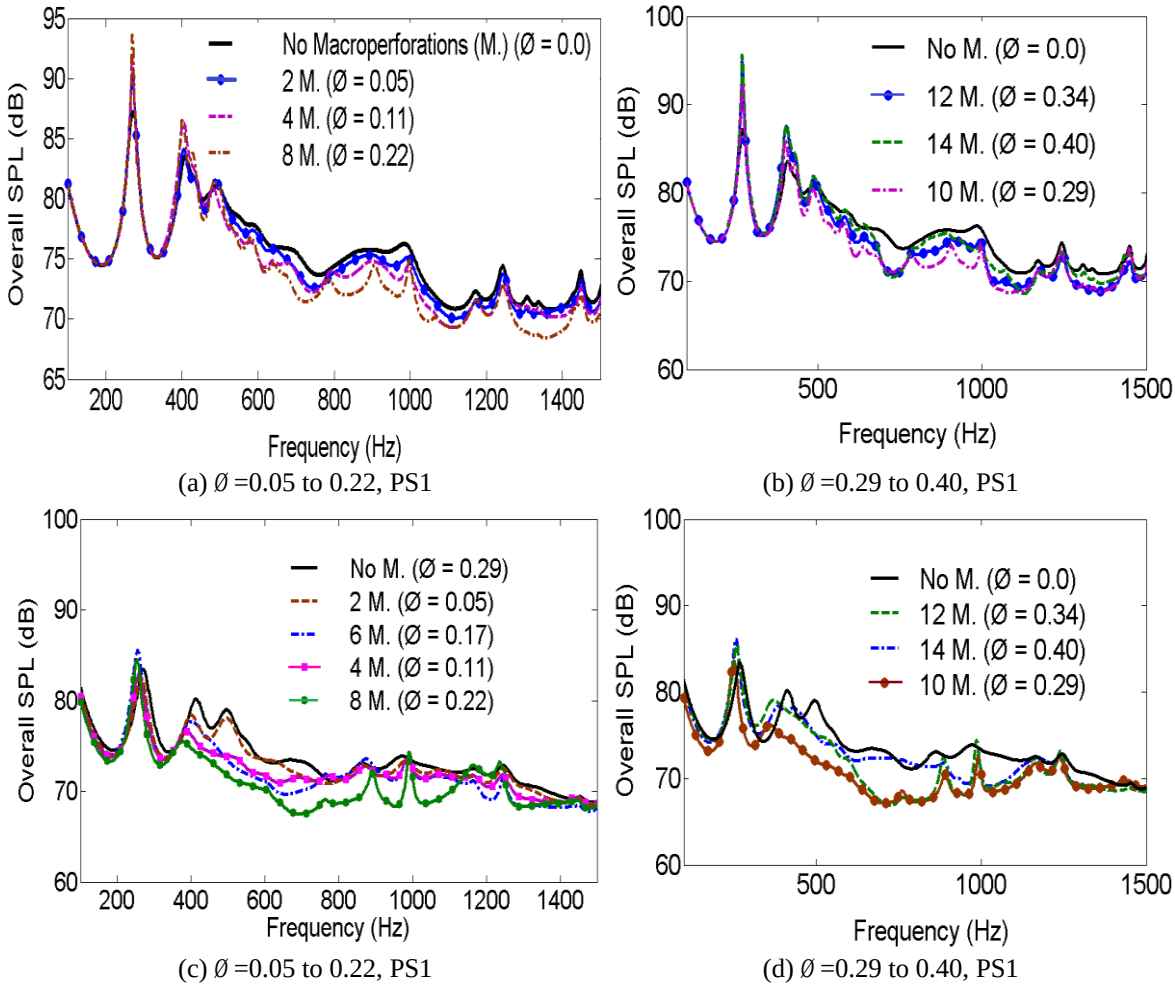

(a) Ø =0.05 to 0.22, PS1

(b) Ø =0.29 to 0.40, PS1

(c) Ø =0.05 to 0.22, PS1

(d) Ø =0.29 to 0.40, PS1

Fig. 8 Comparison of overall SPLs with glasswool layer with varying macroporosity: 80 mm thickness

analysis is carried out to examine the effect of variation of macroporosity on SPL inside the acoustic cavity over a frequency range of 100 Hz to 1600 Hz. The variation in macroporosity is considered from 0.04 to 0.40 for this analysis. Initially, two macroperforations are made at the extreme corners of the poroelastic layer (M=2, Ø =0.057) and with this the overall SPL inside the acoustic cavity is calculated. Further macroperforations are added at the opposite corners (M=4) making macroporosity Ø =0.11; such a sequence is followed with 6, 8 and 10 macroperforations (M=6, 8, 10) producing macroporosity Ø =0.17, Ø =0.22 and Ø =0.29. For 40 mm thickness 1 to 3 dB reduction is achieved with PS1 for macroporosity (Ø) upto 0.35 which is shown in Figs. 8 (a) and (b). Figs. 8 (c) and (d) show a comparison of SPL inside the cavity for these macroporosity (Ø) values for 80mm thickness with PS1. It is clear from the figures that upto macroporosity Ø =0.17, 1 to 3 dB reduction in SPL is achieved and with further increase in macroporosity upto Ø =0.35, 2 to 5 dB reduction is achieved for 80 mm thickness. It is also clear from these figures that 80 mm thickness shows a better reduction in SPL as compared to 40 mm thickness. So for further analyses with PS2, SPLs are calculated only for 80 mm thickness. Figs. 8 (e) and (f) show

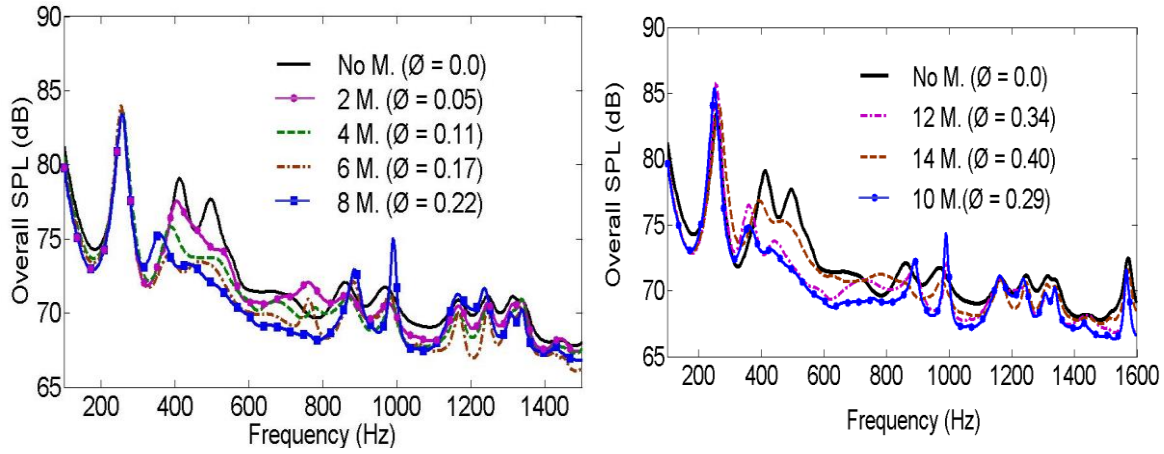

(e) Ø =0.05 to 0.22, PS2 (f) Ø =0.29 to 0.40, PS2

Fig. 8 Continued

the SPLs inside the cavity with PS2 for the same macroporosity values. Irrespective of thickness, beyond the value of macroporosity of 0.35, reduction in SPL goes on diminishing and tends to reach that obtained with a poroelastic layer without any macroperforations.

So it is clear that mode shape based macroperforations enhance the noise reduction inside the acoustic cavity upto a certain range of macroporosity value and this reduction in overall SPL becomes significant with increase in thickness of poroelastic layer. It can be observed from Fig. 8 that reductions in SPL are less for 40 mm than for 80 mm thickness.

4.2 Effectiveness of mode shape based macroperforations over periodic and nodal line based macroperforations

The effect of variation of macroporosity in poroelastic layer on overall SPL is studied. It can be observed from Fig. 8 that macroperforation Pattern 5 with M=10, Ø =0.29 (refer Fig. 7 for all patterns) yields best noise reduction. This pattern is based on pressure mode shapes of the acoustic cavity. Further, macroperforations are made based on nodal lines of the acoustic mode shapes (Pattern 10, M=10, Ø =0.29) and periodic removal (Pattern 9, M=10, Ø =0.29). It is to be noted that these patterns have the same macroporosity as Pattern 5 (M=10, Ø =0.29). The SPLs are calculated using Patterns 9 and 10 and compared with those of Pattern 5. Next, Fig. 9 shows a comparison of SPLs inside the acoustic cavity with glasswool layer of 80mm thickness without any macroperforations and with Patterns 5, 9 and 10 when the acoustic cavity is excited with PS1. The results show that for the same value of macroporosity (M=10, Ø =0.29), better noise reduction is achieved with macroperforations based on mode shape than those based on periodic removal or mode shape nodal lines. Further a different value of macroporosity (M=6, Ø =0.17) is taken with periodic removal (Pattern 8, M=10, Ø =0.17, refer Fig. 7) and mode shape based removal (Pattern 3, M=6, Ø =0.17). Fig. 9 shows a comparison of SPLs with Pattern 8 (6 periodic macroperforations, M=6) and Pattern 3 (6 modeshape based macroperforations, M=6). From Fig. 9, it is clear that Pattern 3 (modeshape based macroperforations) gives better noise reduction than Pattern 8 (periodic macroperforations).

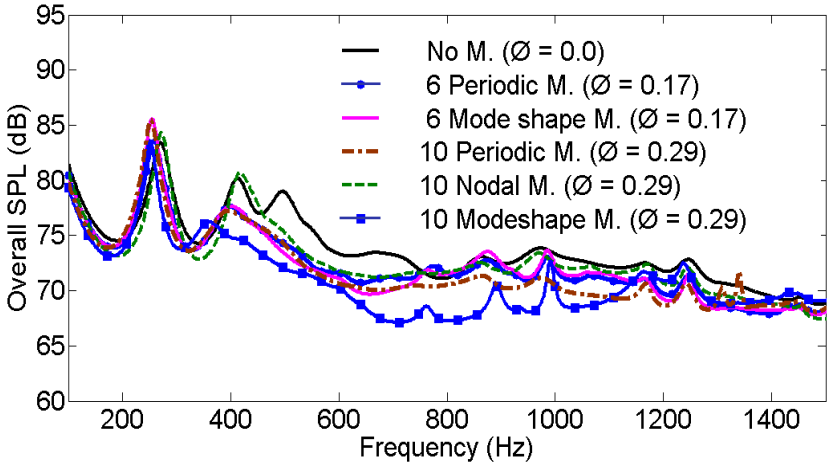

Fig. 9 SPLs for different patterns with same macroporosity and PS1

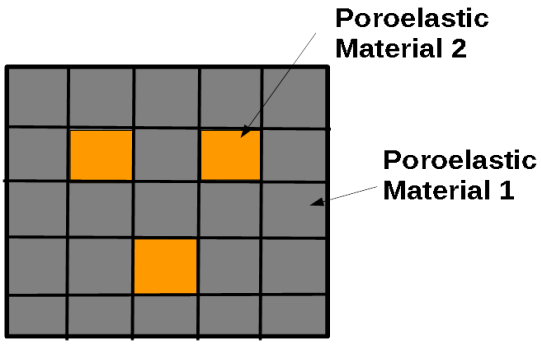

Fig. 10 Double porosity material

This confirms that macroporosity based on mode shapes is more effective in reducing SPL inside the acoustic cavity than that based on periodic removal or macroperforations on mode shape nodal line.

4.3 Effectiveness of mode shape based double porosity over double layered poroelastic materials

The nonhomogeneous double porosity materials are obtained by replacing air filled macroperforations by a different poroelastic material having distinct physical properties (such as different porosity, flow resistivity, etc.). A typical single layer double porosity material is shown in Fig. 10.

The effectiveness of nonhomogeneous poroelastic material layers in terms of sound absorbing coefficients has been demonstrated by Atalla *et al.* (2001). The present paper investigates the effectiveness of double porosity nonhomogeneous material over double layer homogenous material. Different materials having distinct physical properties (Table 1) have been considered for this analysis.

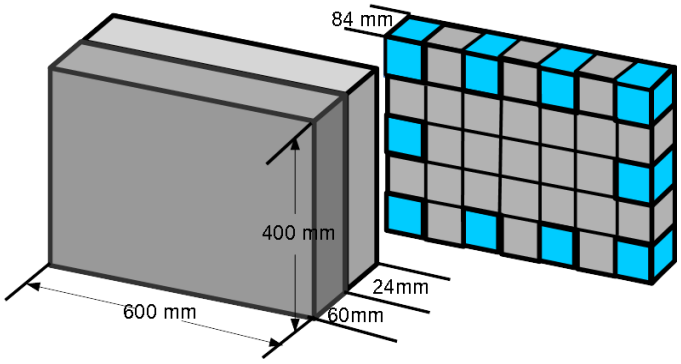

Fig. 11 Volume equivalent double porosity and double layer material

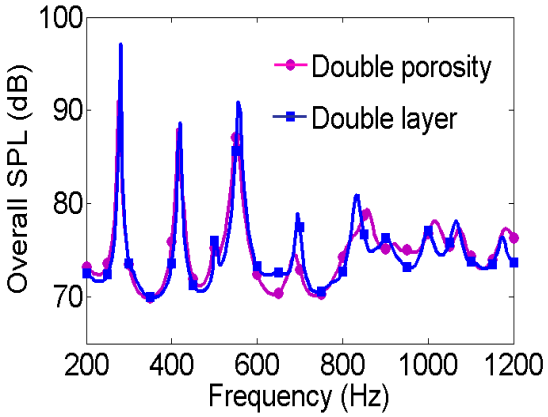

(a) 21 mm thickness (glasswool and fibreglass)

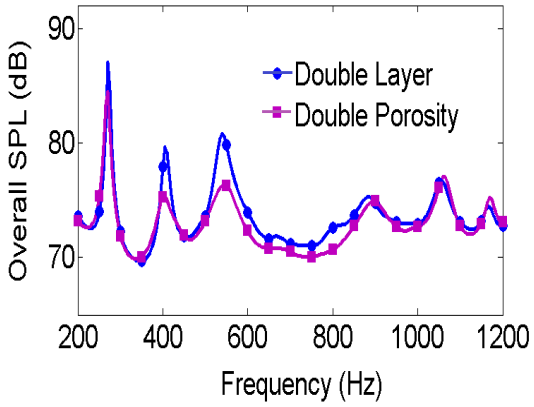

(b) 42 mm thickness (glasswool and fibreglass)

Fig. 12 Comparison of overall SPL obtained using equivolume porosity and double layer material

4.3.1 Double porosity (nonhomogenous single layer) and double layer poroelastic materials

The effect of variation of macroporosity in poroelastic layer on overall SPL is studied. It can be observed from Fig. 8 that macroperforation Pattern 5 with M=10, $\emptyset$=0.29 (refer Fig. 7 for all patterns) yields best noise reduction. This pattern is based on pressure mode shapes of the acoustic cavity. This single layer macroperforated poroelastic material can be converted into nonhomogeneous double porosity material by filling macroperforations with a different poroelastic material. The single layer glasswool (as a base material) is converted into double porosity glasswool fibreglass material by filling the macroperforations using fibreglass (as a filling material) as shown in Fig. 11. The double porosity can be restructured into equivolume homogeneous double layered poroelastic material as shown in Fig. 11. In order to explain this, let us consider an 84mm thick, Pattern 5 macroperforated glasswool layer which has M=10 and $\emptyset$=0.29. It is to be noted that this glasswool layer is divided into 35 equal rectangles. This double porosity single layer nonhomogeneous material is restructured into 60mm glasswool and 24mm fibreglass double layer homogeneous poroelastic material keeping the volume constant. This can be explained by the following two mathematical calculations: $84\times25=(x)\times35\Rightarrow x=60$ and $84\times10=(x)\times35\Rightarrow x=24$.

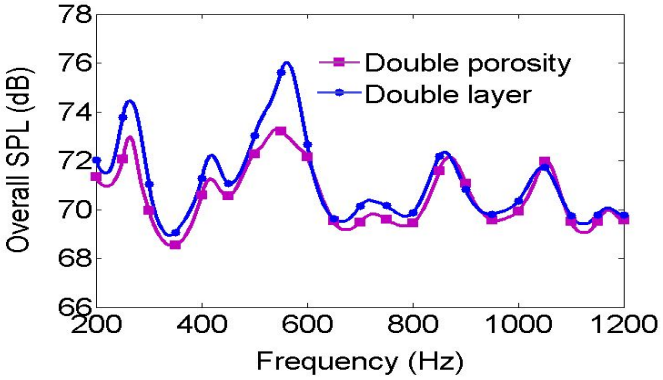

Fig. 13 Comparison of overall SPL obtained using equivalent 84 mm thick double porosity and double layer material

So, it is worth noting that 84mm double porosity material can be restructured into equivolume double layer homogeneous material of 60 mm base and 24 mm thick filling material. On a similar basis, 42 mm double porosity material can be restructured into equivolume double layer homogeneous material of 30 mm base and 12 mm thick filling material and also 21 mm double porosity into 15 mm base and 6mm filling double layer poroelastic material. This addition of a different material alters stiffness and mass characteristics of the system which makes double porosity materials more effective compared to equivalent double layer poroelastic materials.

Comparison of overall SPL obtained with equivalent double porosity and double layer poroelastic material

The overall SPL is obtained by using these equivolume double porosity and double layer poroelastic materials of 21 mm and 42 mm thicknesses, which is shown in Fig. 12.

For this analysis, the acoustic cavity is discretized into 7×7×5 and poroelastic material domain is discretized into 7×7×5 and the system is excited with the point source PS3 having coordinates 0.25,0.25 and 0.24 along *X*, *Y* and *Z* directions respectively. For 21 mm thickness, nearly equal overall SPL is obtained for both double porosity and double layer poroelastic materials. For 42 mm thickness double porosity material seems to be effective in the range of 400 Hz to 900 Hz compared to equivalent double layer poroelastic material; however the reduction obtained is not significant as seen in Fig. 12(b). From Fig. 12(a) and 12(b), it is clear that double porosity materials are more effective in reducing SPL inside the acoustic cavity compared to equivalent double layer materials having the same volume and this effectiveness goes on increasing with increase in the thickness of poroelastic material layer. This observation is confirmed from Fig. 13 in which comparison of SPL obtained with equivalent 84mm double layer and double porosity material is shown. From Fig. 13 it is clear that a notable reduction in SPLs is obtained for 84mm thickness with double porosity as compared to double layer poroelastic material.

Comparison of overall SPL obtained using double porosity material with different filling material

Effectiveness of double porosity material over equivalent double layer poroelastic material (having equal total volume) in terms of SPL is investigated. Further, different filling materials such as foams are used to investigate the effectiveness of double porosity materials over equivalent

double layer materials. Fig. 14 shows a comparison of SPL obtained with double poroelastic materials with different filling materials (foam A and foam B instead of fibreglass). It is clear from Fig. 14 that a combination of glasswool and fibreglass (double porosity material) produces the least SPL among the combination of glasswool and foam A or foam B. It is worthwhile noting that fibreglass has low flow resistivity compared to foam A or foam B (refer Table 1). It can be stated that when low flow resistivity material is used to fill macroperforations of the poroelastic material layer to make double porosity material corresponding double porosity material yields better noise reduction compared to that obtained with a different filling material which has high flow resistivity.

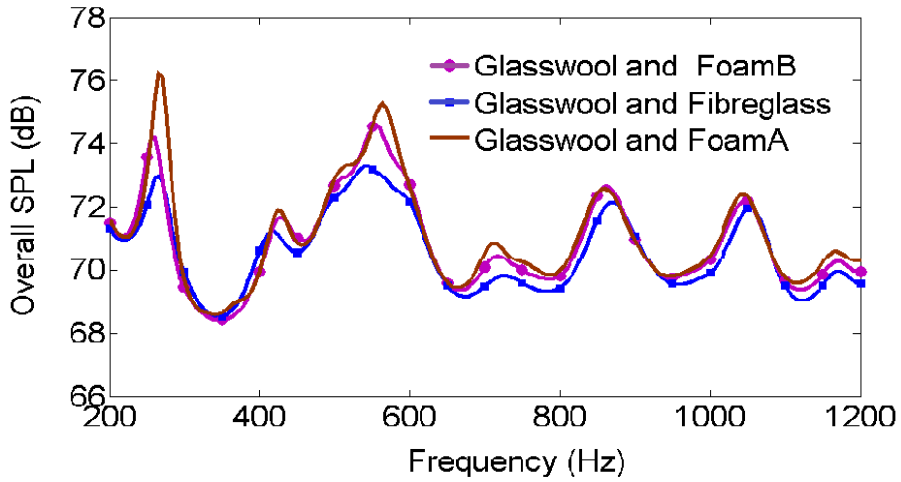

Fig. 14 Comparison of overall SPL obtained for different filling materials

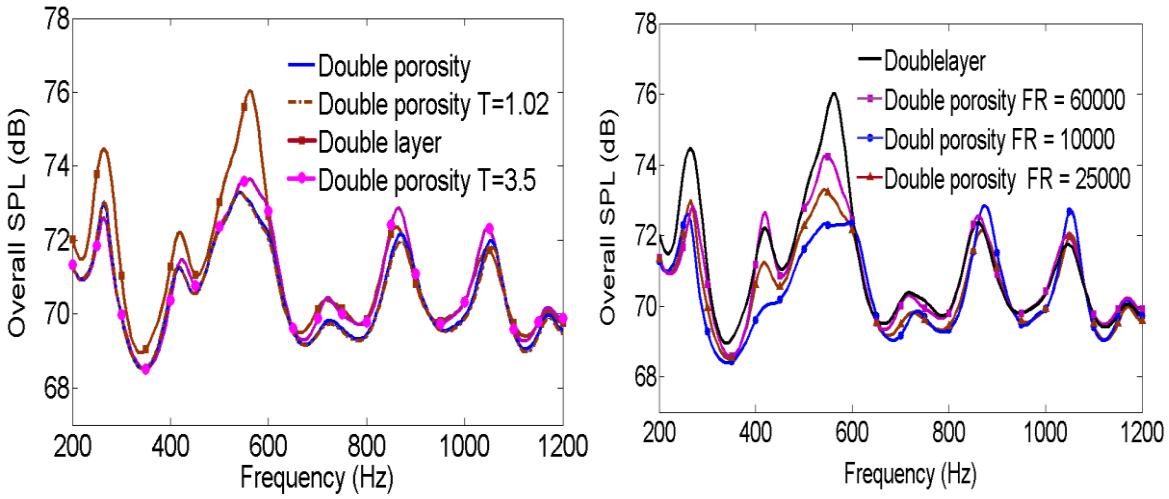

(a) Altered tortuosity (glasswool and fibreglass) (b) Altered flow resistivity (glasswool and fibreglass)

Fig. 15 Comparison of overall SPL obtained using 84 mm double porosity material with altered physical properties of filling material

Comparison of overall SPL obtained using double porosity material with altered properties of fibreglass (filling material)

In the two earlier sub sections, effectiveness of double porosity material over equivalent double layer poroelastic material (having equal total volume) in terms of SPL has been investigated, followed by a similar analysis with different filling materials which have distinct physical properties. In this subsection, the physical properties such as tortuosity and flow resistivity of fibreglass materials which are used to fill the macroperforations are altered and consequently their effect on SPL is investigated. Fig. 15 shows a comparison of SPL obtained with double porosity material (glasswool and fibreglass) with altered physical properties of fiberglass viz., tortuosity (referred to as *T* in Fig. 15(a)) and flow resistivity (referred to as FR in Fig. 15(b)). It is clear from Fig. 15(a) that altered tortuosity of fibreglass does not affect the SPL significantly, however it can be concluded that an increase in tortuosity tends to increase SPL and vice versa. When the flow resistivity of fibreglass is increased, it is observed that it produces SPLs on the higher side; consequently decrease in flow resistivity of fibreglass yields a notable reduction in SPLs compared to the SPLs obtained without any change in material properties of fibreglass.

5. Conclusions

In the present paper, effects of variation of macroporosity and effect of double porosity in poroelastic layer on overall SPL in the acoustic cavity are examined. For this analysis coupled acoustic poroelastic 3-D FE model is used.

It has been shown that macroperforations in poroelastic layers based on acoustic mode shapes enhance noise reduction in the macroporosity range $\emptyset$ =0.20 to $\emptyset$ =0.35. Beyond this value of macroporosity ($\emptyset$ =0.35), reduction in overall SPL diminishes and tends to reach that obtained with a poroelastic layer without any macroperforations and when macroporosity $\emptyset$ =0.4, overall SPL values for different frequency ranges are higher compared to no layer case.

Secondly, macroperforations based on mode shapes of the acoustic cavity yield better noise reduction compared to nodal line based and periodic macroperforations in poroelastic layers.

Finally, it has been shown that double porosity materials obtained by filling the macroperforations based on mode shapes of acoustic cavity are effective in terms of reducing overall SPL compared to equivolume double layer poroelastic materials and such double porosity materials yield better noise reduction when low flow resistivity material is used to fill the macroperforations.

References

Allard, J.F. and Atalla, N. (2009), *Propagation of Sound in Porous Media: Modelling Sound Absorbing Materials*, Wiley, United Kingdom.

Atalla, N., Panneton, R. and Debergue, P., (1998), "A mixed displacement pressure formulation for poroelastic materials", *Acoust. Soc. Am.*, **98**(104), 1444-1452.

Atalla, N., Sgard, F., Only, X. and Panneton, R. (2001), "Acoustic absorption of macro perforated porous materials", *J. Sound Vib.*, **243**(4), 659-678.

Besset, S. and Ichchou, M.I. (2011), "Acoustic absorption material optimization in the mid-high frequency range", *Appl. Acoust.*, **72**(9), 632-638.

Goransson, P. (1995), "A weighted residual formulation of the acoustic wave propagation through a flexible

porous material and comparison with limp material model", *J. Sound Vib.*, **182**, 479-494.
Ih, J.Y., Heo, Y., Cho, S. and Cho W. (2011), "Optimal positioning of sources and absorbing materials for the sound field rendering by array speakers", *Forum Acusticum, 6th Conference*, Denmark, June-July.
Lenin, M.C. and Padmanabhan, C. (2010), "Noise control of rectangular cavity using macro perforated poroelastic materials", *Appl. Acoust.*, **71**, 418-430.
Panneton, R. and Atalla, N. (1997), "An efficient finite element scheme for solving the three dimensional poroelasticity problem in acoustics", *J. Acoust. Soc. Am.*, **101**(6), 3287-3298.
Petyt, M., Lea, J. and Koopmann, G.H. (1976), "A finite element method determining the acoustic models of irregular shaped cavities'', *J. Sound Vib.*, **45**(4), 495-502.
Sgard, F.C., Only, X., Atalla, N. and Castel, F. (2005), "On the use of perforations to improve the sound absorption of porous materials", *Appl. Acoust.*, **66**,625-651.
Totaro, N. and Guyader, J. (2011), "Efficient positioning of absorbing material in complex systems by using the Patch Transfer Function method", *J. Sound Vib.*, **331**(2012), 3130-3143.
Zienkiewicz, O.C. and Taylor, R. (1989), *The Finite Element Method*, Mcgraw-Hill, London